LIMNOLOGY
and
OCEANOGRAPHY

ASLO

Limnol. Oceanogr. 60, 2015, 1562–1576

doi: 10.1002/lno.10117

Responses of the coastal phytoplankton community to tropical cyclones revealed by high-frequency imaging flow cytometry

Sílvia Anglès,*[1,2] Antoni Jordi,[2] Lisa Campbell[1]

[1]Department of Oceanography, Texas A&M University, College Station, Texas, United States of America
[2]Departament d'Ecologia i Recursos Marins, Institut Mediterrani d'Estudis Avançats, IMEDEA (UIB-CSIC), Esporles, Mallorca, Spain

Abstract

To investigate the response of a subtropical coastal phytoplankton community to tropical cyclones, we utilized high temporal resolution (hours) data from the Imaging FlowCytobot (IFCB) deployed in the Gulf of Mexico. In 2010, four tropical cyclones (two during June–July and two during September) struck the area. Passage of the cyclones produced two major impacts: (1) storm surges and strong onshore winds, and (2) heavy rains producing substantial freshwater discharge and decreased salinity. The phytoplankton community showed a rapid response to the passage of the cyclones with increased abundance. Using principal component analysis, responses during storm surges and after freshwater discharges were distinguished and considerable changes in community composition were revealed. Responses to storm surges were characterized by an increase of diatoms. Freshwater discharges triggered increases in dinoflagellates and other flagellates (prasinophytes, euglenophytes, and cryptophytes) relative to the other groups. In June–July, substantial increases in diatoms were also observed. The response to freshwater discharge during this period was dominated by a diatom (*Thalassiosira*), whereas in September the response was dominated by two dinoflagellates (*Akashiwo sanguinea* and *Polykrikos hartmannii*). Observed abundances of these three taxa were the highest recorded from the IFCB time series. The short-term responses of the phytoplankton community revealed here emphasize the need for high temporal resolution sampling to fully capture the effects of tropical cyclones. Given that extreme storms are predicted to increase with future climate change, the taxonomic resolution of the IFCB is also valuable for detecting taxa-specific responses, which can have implications for ecosystem functioning.

Episodic climatic events such as droughts, floods, or storms cause profound and multifaceted impacts on aquatic ecosystems ultimately altering their structure and function. Morevover, such events are expected to intensify in frequency and magnitude due to global climate change (Meehl et al. 2007). Tropical cyclones, such as hurricanes, typhoons, tropical storms or tropical depressions, are extreme storms that produce environmental perturbations with substantial effects in physical and chemical conditions. Perturbations associated with tropical cyclones include alteration of tidal regimes, upwelling, vertical mixing, sediment resuspension, and terrestrial runoff that affect estuaries, coastal areas and the open ocean (Shiah et al. 2000; Babin et al. 2004; Wetz and Yoskowitz 2013). The extent of these impacts is dependent upon storm magnitude in terms of intensity (i.e., amount of wind and precipitation), duration and location, as well as upon environmental conditions of the system before and after the passage of the cyclone (e.g., degree of stratification and nutrient concentration). In addition, the physical nature of the system (i.e., geometry and topography) can influence the response (Mallin et al. 2002; Mallin and Corbett 2006; Wetz and Paerl 2008b).

Considerable effort has been devoted to investigating the impacts of tropical cyclones on phytoplankton in marine ecosystems. Phytoplankton are the main source of primary production supporting food webs in these systems and play an essential role in biogeochemical cycling. Therefore, characterization of the processes that influence phytoplankton communities and of the consequent responses is crucial for understanding ecosystem functioning. In the continental shelf and in the open ocean, wind-forced upwelling, water mixing and sediment resuspension, and occasionally riverine nutrients can enhance nutrient concentrations that lead to increases in phytoplankton biomass (Shiah et al. 2000; Lin et al. 2003; Babin et al. 2004; Yuan et al. 2004; Hu and

Additional Supporting Information may be found in the online version of this article.

*Correspondence: sangles@tamu.edu; angles.silvia@gmail.com

Muller-Karger 2007). In estuaries, wind-driven water mixing and sediment resuspension can induce nutrient entrainment to the water column by disrupting the stratification and resuspending nutrients (e.g., Paerl et al. 2006b; Wetz and Paerl 2008b). In addition, tropical cyclones can produce substantial input of nutrients and organic matter through freshwater river discharges as a result of precipitation that can trigger phytoplankton blooms and shifts in the community composition (Mallin et al. 1993). However, the high turbidity and reduced water residence times often associated with terrestrial runoff can also generate conditions that are unfavorable for phytoplankton growth (e.g., low light and rapid flushing; Paerl et al. 1998; Peierls et al. 2003).

Phytoplankton responses to tropical cyclones in estuaries, the continental shelf and the open ocean can be on the order of days to several weeks (Fogel et al. 1999; Lin et al. 2003; Babin et al. 2004; Wetz and Yoskowitz 2013). In estuarine systems, long-term effects (months–years) after the passage of intense hurricanes have also been documented (Paerl et al. 2001; Peierls et al. 2003), although considerable phytoplankton responses can occur on the order of days during relatively weak tropical cyclones (Wetz and Paerl 2008*b*; Paerl et al. 2010). Alterations of the environmental conditions caused by tropical cyclones occur rapidly; consequently, rapid shifts in the phytoplankton community structure affect the responses of the associated food web components (Zhang and Wang 2000; Wetz and Paerl 2008a). However, most sampling programs are not designed to capture short-term (hours–days) changes in the phytoplankton community structure. Thus, the short-term response of phytoplankton to these events and the potential consequences to ecosystem functioning remain largely unknown. Considering the episodic nature of tropical cyclones and their predicted increase under the future global change scenario, studies characterizing the short-term phytoplankton response are needed to fully understand the impact of these climatic perturbations on ecosystem functioning.

The phytoplankton time series at the Texas Observatory for Algal Succession Timeseries (TOAST) is located at the entrance of the Mission-Aransas estuary, a subtropical coastal ecosystem in the Gulf of Mexico. Using the Imaging FlowCytobot (IFCB; Olson and Sosik 2007) continuous automated images of the phytoplankton community at high temporal resolution (hours) are generated (Campbell et al. 2010, 2013; Henrichs et al. 2011). In addition to the high temporal resolution, the IFCB time series offers other advantages with respect to prior studies. It allows for the characterization of the phytoplankton community to genus or species level. Phytoplankton groups show different responses to environmental changes as a result of their particular requirements (e.g., nutrients), often at the species level (Reynolds 2006). Moreover, selective grazing pressure on particular groups or species may affect trophic transfers in the food web and biogeochemical cycling. Thus, evaluation of the changes in phytoplankton community composition can provide a more detailed understanding of ecosystem functioning. The location of TOAST in a subtropical coastal ecosystem also provides the occasion to examine the effects of tropical cyclones in an environment particularly sensitive to such episodic perturbations. Due to the limited seasonality in light and temperature, temporal patterns of phytoplankton abundance in subtropical systems are often more influenced by variations in climatic conditions (e.g., episodic freshwater discharges, tropical cyclones, droughts) than by seasonality compared to temperate ecosystems (Murrell et al. 2007; Phlips et al. 2012). Indeed, the dynamics of primary producers, higher trophic levels and biogeochemical cycling are more tightly coupled (Hoover et al. 2006; Murrell et al. 2007; Bruesewitz et al. 2013). Therefore, the relevant time scale in these ecosystems can be of hours to days, for which the high temporal resolution of the IFCB time series is important.

In 2010, a sequence of four tropical cyclones (Hurricane Alex, Tropical Depression Two, Tropical Storm Hermine, and Hurricane Karl) occurred in the Gulf of Mexico. The IFCB time series at TOAST provided an unprecedented opportunity to investigate the responses of the coastal phytoplankton community to tropical cyclones with high temporal resolution (hours). The IFCB time series together with high frequency measurements of physical and hydrological variables were analyzed to identify and characterize changes in the phytoplankton community. Our aim was to improve our knowledge on how tropical cyclones affect phytoplankton communities at the relevant time scales.

Methods

Study area

The study area encompasses several estuarine systems of the Western Gulf of Mexico (Texas): the Guadalupe, Mission-Aransas and Nueces estuaries and the primary inlet that connects these systems to the Gulf of Mexico, the Aransas Pass (Fig. 1). Water enters the Aransas Pass from the Gulf of Mexico through three channels (Corpus Christi Ship Channel, Lydia Ann Channel and Aransas Channel). The estuaries are hydraulically connected through the Gulf Intracoastal Waterway, and Aransas Pass receives freshwater inflow from several rivers discharging in the estuarine systems (Orlando et al. 1993). The estuarine systems are shallow ($\sim$ 1-3 m average depth). The water column is typically well mixed throughout the year (Brown et al. 2000). In addition to tides, winds > 7 m s^{-1} can cause sediment resuspension in the area (Wynne et al. 2005). The estuarine systems are usually nitrogen (N) limited (Pennock 1999; Mooney and McClelland 2012). Although few studies have analyzed the phytoplankton community in the Nueces and Mission-Aransas estuaries, Holland et al. (1975) reported that the community composition was uniform throughout the bays,

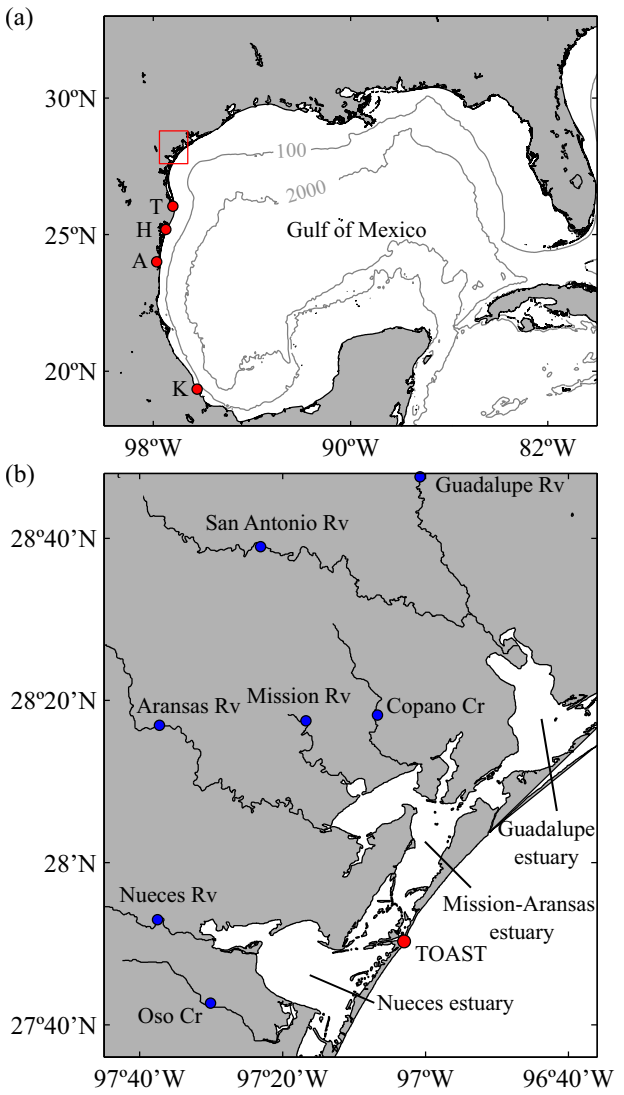

Fig. 1. Location of: (a) the study area (red square) and landfall of Hurricane Alex (A), Tropical Depression Two (T), Tropical Storm Hermine (H) and Hurricane Karl (K) (red dots); and (b) TOAST in the Port Aransas Ship Channel (red dot) and the rivers of the estuarine system, with the USGS stream gauge stations (blue dots). [Color figure can be viewed in the online issue, which is available at wileyonlinelibrary.com.]

slightly influenced by the salinity regimes in the different parts of the estuaries.

Imaging FlowCytobot time-series data

Phytoplankton community composition data were acquired with the IFCB, which combines flow cytometry and video technologies to capture images of nano- and microplankton (> 10 to ~ 150 μm) and the associated fluorescence and light scattering signals (Olson and Sosik 2007). Since September 2007, the IFCB has been deployed at the TOAST site on the University of Texas Marine Science Institute pier, located in the Port Aransas Ship Channel in Aransas Pass, Texas (27° 50.296′ N, 97° 3.017′ W; Fig. 1b). This station is part of the Mission-Aransas National Estuarine Research Reserve (NERR) System Wide Monitoring Program. The Port Aransas Ship Channel is a well-mixed channel with strong tidal currents. Tidal range is ~ 1.0 m and the average water depth is 6.5 m. Water temperature ranges from 7.1°C to 32.1°C (average 23°C) and salinity ranges from 12.6 to 41.3 (average ~ 32.2).

Tidal velocity ranges from -1.5 m s^{-1} to -1.8 m s^{-1}, where negative values indicate water movement into the channel (Harred and Campbell 2014). The location of the IFCB at the entrance to the estuary allows characterization of the plankton community of both estuarine and coastal waters as the water flow moves from the estuaries to the sea (outgoing tide) and moves from the sea into the estuaries (incoming tide).

The IFCB collects a 5 mL sample of near-surface water every ~ 20 min. It runs continuously, although in the time series used for this study there are a few gaps (usually ~ 1 d) due to electrical power failures caused by the cyclones or for maintenance. Image files are processed and classified automatically following the approach described by Sosik and Olson (2007), with the modification of replacing the support vector machine with an assemblage of decision trees obtained by the random forest approach of Breiman (2001). For this study, the automated classifier used to classify the data had 53 categories that represented the community composition of phytoplankton and microzooplankton of the study area (Supporting Information Table S1). Categories were defined by morphology, so were either genus- or species-specific or groups of taxa with similar morphological characteristics. The classifier included 21 categories of diatoms, 11 categories of dinoflagellates, 7 categories of other phytoplankton groups, the category Other cells (small cells that cannot be taxonomically identified from the images), 11 categories of microzooplankton, and a detritus category (noncellular material).

A training set for the automated classification was produced with 300 images for each category selected at random from the image data set spanning from 2007 to 2010. An optimized threshold of classification probability score from the random forest approach was determined for each category. The thresholds minimized residuals between manual and classifier-based abundance estimates. To evaluate the accuracy of the automated classification, randomly selected files from the 2007-2012 image data set were classified manually. A total of 106,383 images were visually inspected and manually placed into their corresponding categories (at least 150 images for category). Manual and automated results were compared and a correction of abundance estimates was applied as described in Sosik and Olson (2007). Overall, the automated classification and correction accuracy across all 53 categories was 77%.

Estimation of cell abundance of chain-forming diatoms was performed as described in Olson and Sosik (2007). The

number of cells per chain was counted in images for every chain-forming diatom category; reprentative images were selected to cover the range of chain length as much as possible. The measured duration of chlorophyll fluorescence signal in each chain was calibrated with the corresponding manual cell count to obtain estimations of cell abundances over the entire time series.

Meteorology, hydrology, and physical variables

To characterize the spatial distribution and the temporal evolution of the four tropical cyclones, we used 10-m wind and sea-level atmospheric pressure fields from the European Centre for Medium-Range Weather Forecasts ERA-Interim reanalysis (Dee et al. 2011). Meteorological and hydrological data from stations near the IFCB (< 1 km) were used to assess the local effects of the cyclones. Precipitation data were taken from the National Oceanic and Atmospheric Administration's (NOAA) National Weather Service (station Mustang Beach Airport; http://www.weather.gov/). Sea level and salinity were obtained from the Mission-Aransas NERR website from the Port Aransas Ship Channel station (http://cdmo.baruch.sc.edu/). Current velocity data were downloaded from the Texas A&M University Corpus Christi Division of Nearshore Research website (http://lighthouse.tamucc.edu/) from the Real-Time Navigation System Station located on the Port Aransas Ship Channel station. Tidal sea level and currents were estimated from sea level and current velocity data by an iteratively reweighted least-squares calculation of harmonic analysis (Leffler and Jay 2009). Freshwater discharges to the estuary system were compiled from the U.S. Geological Survey (USGS) database from stream gauge stations that where more closely located to the estuaries (Guadalupe river, station 08176500; San Antonio river, station 08188500; Copano creek, station 08189200; Mission river, station 08189500; Aransas river, station 08189700; Nueces river, station 08211500; Oso creek, station 08211520; Fig. 1b).

Data analysis

Of the 53 categories in the classifier, only 23 categories were included in the data analysis (*see* Supporting Information Table S1); the remaining phytoplankton categories were generally absent, or if present, they appeared sporadically and at very low abundances. Hourly data for each of these 23 categories were used to characterize the responses of the phytoplankton community over the study period. Because this data set is too large for direct visualization and analysis, a method to encode the time series of the different categories into a smaller set of numbers is necessary. This can be accomplished using principal component analysis (PCA), which is a common exploratory multivariate statistical technique (Hotelling 1933). The mathematical basis of the PCA technique is provided in the Supporting Information. The PCA was applied to hourly averaged and standardized data from the 23 categories over the entire time series (data from 2008 to 2012). The PCA decomposes data into the patterns (components) that explain most of the variation of the different phytoplankton categories, which allows identification of the phytoplankton community responses over the course of the tropical cyclones.

To determine if the observed increases in abundance were consistent with potential cell growth in response to environmental stimulation driven by the cyclones, estimates of growth rates were calculated for each of the categories that dominated the responses identified by the PCA. Category-specific growth rates were calculated as the logarithm of the difference in cell abundance between the maximum peak of the category and the onset of the stimulation process divided by the time interval between these points.

Results

Tropical cyclones description

In 2010, four tropical cyclones occurring in the Gulf of Mexico had substantial impact in the study area within a 12-week period. Landfall locations are indicated in Fig. 1a. Tropical cyclones were concentrated in two periods, June–July and September (Fig. 2). The first cyclone of June–July was Hurricane Alex, which moved from the southwestern Gulf of Mexico on 28 June toward the north-northwest while gradually intensifying. Alex made landfall in northeastern Mexico as a strong Category 2 hurricane on 01 July and rapidly weakened over land on 02 July. The second cyclone of June–July was Tropical Depression Two, formed ~ 1 week after Alex over the western Gulf of Mexico from a tropical wave and made landfall on 08 July. During September, the first cyclone was Tropical Storm Hermine, which developed over the southwestern Gulf of Mexico on 06 September. Hermine moved north and made landfall on the coast of northeastern Mexico on 07 September. After 10 d Hurricane Karl, the second September cyclone, emerged over the southern Gulf of Mexico as a strong Category 3 hurricane on 16 September. Karl made landfall on 17 September on the eastern coast of Mexico (relatively far from the study area).

Hydrological and physical conditions

As a consequence of the strong onshore winds along the Texas coast, storm surges developed in Port Aransas Ship Channel and adjacent estuarine systems during the passage of each pair of tropical cyclones (Figs. 3a, 4a). The magnitude of the storm surge was related to the intensity of the tropical cyclone; thus, storm surge was greater for hurricanes Alex and Karl (~ 0.62 m and ~ 0.38 m, respectively) than Two and Hermine (~ 0.36 m and ~ 0.18 m, respectively). After the passage of the tropical cyclones, the sea level gradually recovered.

The tropical cyclones also brought heavy rains to a large portion of southern Texas. At the station nearest to TOAST, the total accumulated precipitation recorded was 108.2 mm, 25.1 mm, 152.4 mm, and 334.5 mm for Alex, Two, Hermine

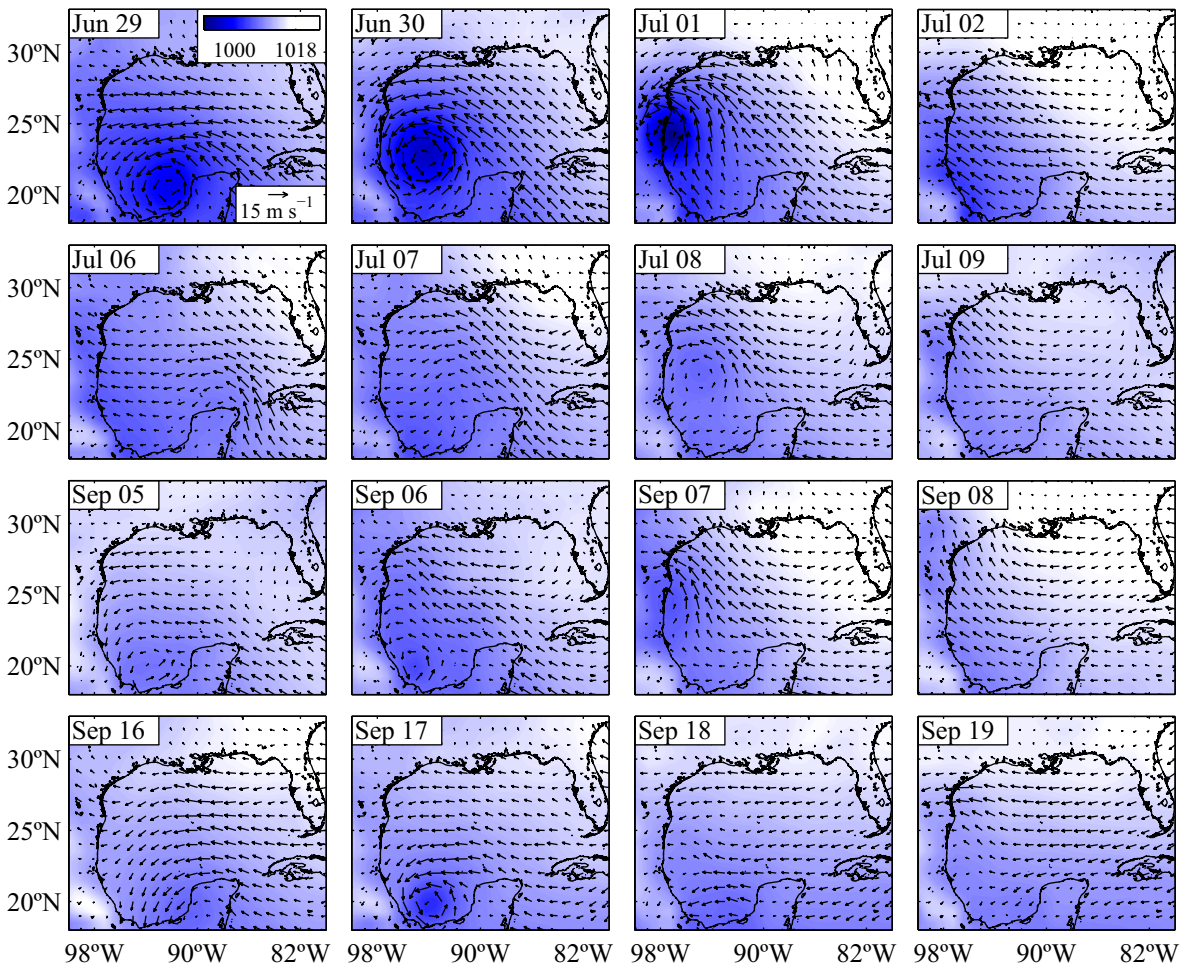

Fig. 2. Spatial distribution and temporal evolution of the tropical cyclones in the study area in 2010: wind directions and speed (arrows) and sea-level pressure (color bar). From top to bottom: Hurricane Alex, Tropical Depression Two, Tropical Storm Hermine and Hurricane Karl. [Color figure can be viewed in the online issue, which is available at wileyonlinelibrary.com.]

and Karl, respectively (Figs. 3b, 4b). As a result, freshwater discharge recorded at the USGS stations increased. During June–July, peak daily mean streamflow reached 290 m^3 s^{-1} after Alex, sixfold greater than baseline streamflow before the hurricane's passage (Fig. 3b). Average daily mean streamflow after Alex was 145 m^3 s^{-1}. Freshwater discharge declined gradually during the following days until the second tropical cyclone (Two) occurred. Despite the low precipitation recorded, Two produced moderate freshwater discharge, with average and peak daily mean streamflows of 131 m^3 s^{-1} and 257 m^3 s^{-1}, respectively. During September, Hermine caused large freshwater runoff, with peak daily mean streamflow of 490 m^3 s^{-1} following its passage, 16-fold greater than baseline streamflow before the passage of the tropical storm (Fig. 4b). Average daily mean streamflow after Hermine was 208 m^3 s^{-1}. Hurricane Karl also produced substantial freshwater discharge. Average and maximum daily mean streamflow reached 199 m^3 s^{-1} and 474 m^3 s^{-1}, respectively.

Freshwater discharge caused a consequent salinity decrease at the study site (Figs. 3c, 4c). In June–July, salinity started to decline gradually from 35 since the passage of Alex reaching a minimum of 23 after Two (Fig. 3c). Then, salinity recovered progressively to baseline values in $\sim$ 6 d. The impact of the freshwater discharge in September was greater. As a result of the combined freshwater discharge after Hermine and Karl, salinity decreased dramatically over 23 d and attained minimum values of 21-24 for several days (Fig. 4c). Afterward, salinity remained around 24-26 for $\sim$ 10 d and then increased progressively. The period for salinity recovery to pre-cyclone levels lasted $\sim$ 8 d.

Phytoplankton community responses

The total abundance of phytoplankton cells showed marked responses to the tropical cyclones (Figs. 3d, 4d). In June–July, a progressive increase in the total abundance of phytoplankton cells was observed, which initiated during the passage of Alex (Fig. 3d). Total cells reached the

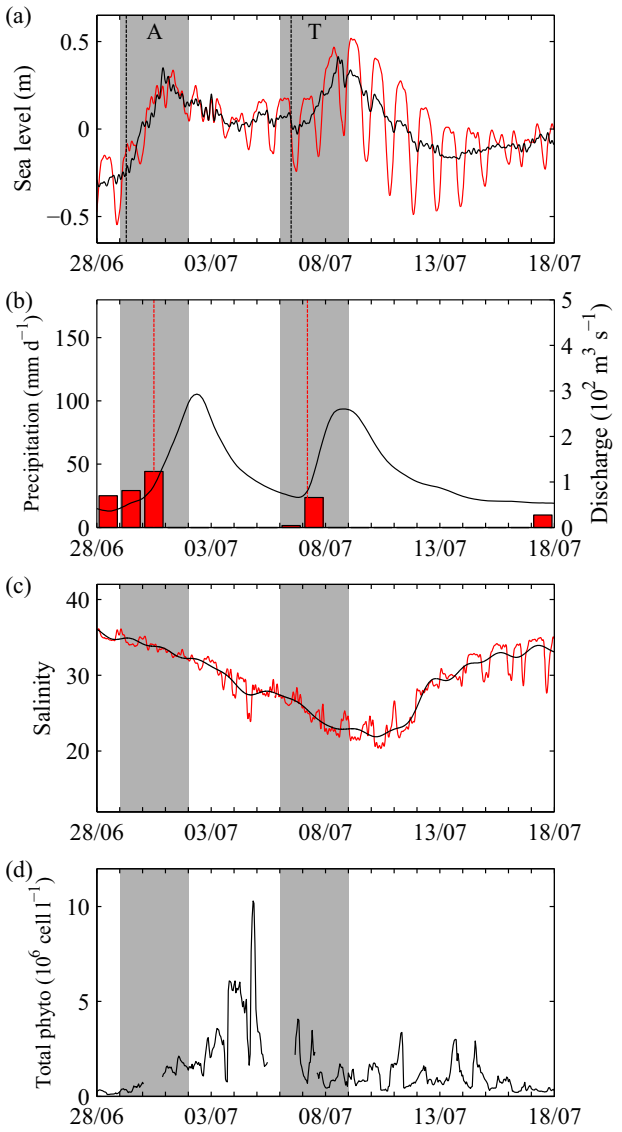

Fig. 3. Hydrological, physical and biological conditions during June–July at TOAST in the Port Aransas Ship Channel: (a) sea level (red line) and de-tided sea level (black line); (b) precipitation (red bars) and total freshwater discharges calculated from the USGS stream gauge stations (black line); (c) salinity (red line) and low-pass filtered salinity (33-h) (black line); (d) total phytoplankton cell abundance. Vertical dashed lines indicate start of the storm surge (black line) and the freshwater discharge (red line) for each tropical cyclone. Grey bars indicate temporal evolution of Hurricane Alex (A) and Tropical Depression Two (T) as in Fig. 2. [Color figure can be viewed in the online issue, which is available at wileyonlinelibrary.com.]

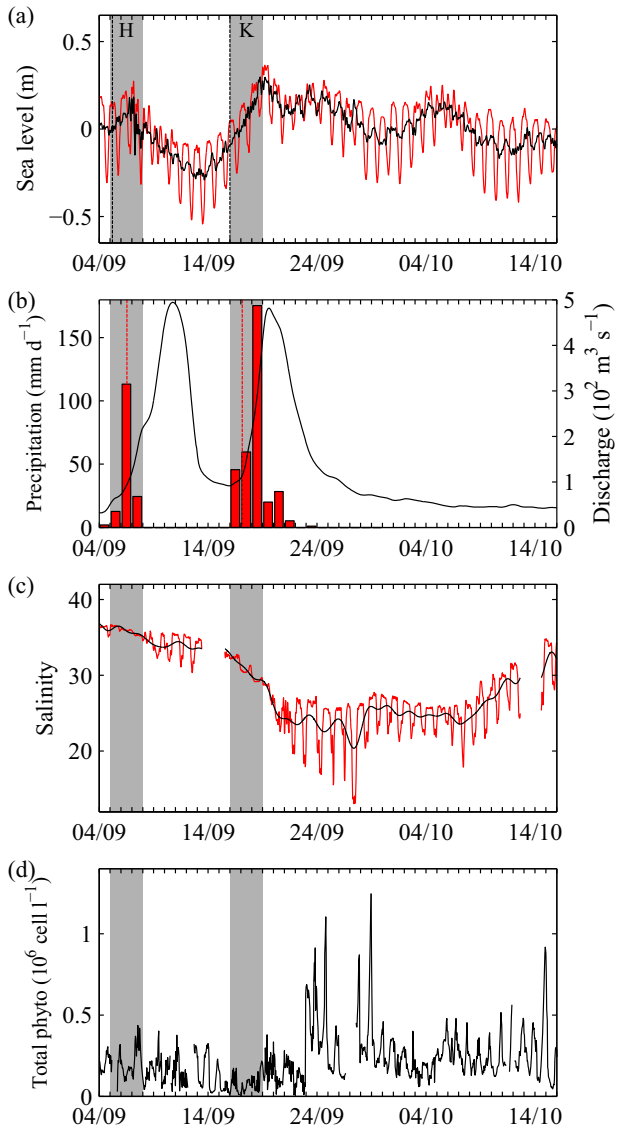

Fig. 4. Hydrological, physical and biological conditions during September at TOAST in the Port Aransas Ship Channel: (a) sea level (red line) and de-tided sea level (black line); (b) precipitation (red bars) and total freshwater discharges calculated from the USGS stream gauge stations (black line); (c) salinity (red line) and low-pass filtered salinity (33-h) (black line); (d) total phytoplankton cell abundance. Vertical dashed lines indicate start of the storm surge (black line) and the freshwater discharge (red line) for each tropical cyclone. Grey bars indicate temporal evolution of Tropical Storm Hermine (H) and Hurricane Karl (K) as in Fig. 2. [Color figure can be viewed in the online issue, which is available at wileyonlinelibrary.com.]

maximum abundance (10.3×10^6 cells L^{-1}) 4.9 d after the increase in freshwater discharge (Fig. 3d). Total cell abundance afterward was lower and variable, showing peaks in abundance during and after the passage of Two. After the period of salinity recovery, abundance decreased until reaching values similar to those before the cyclones. During September, total cell abundances were lower compared to June–July (Fig. 4d; note the different scales for *y* axis in Figs. 3d, 4d). Total abundances showed a modest increase during the passage of Hermine, followed by a slightly decreasing tendency that reached minimum concentrations after the elevated freshwater discharge. Abundances increased abruptly and reached up to 1.2×10^6 cells L^{-1} 12 d after the increase in freshwater discharge caused by Karl.

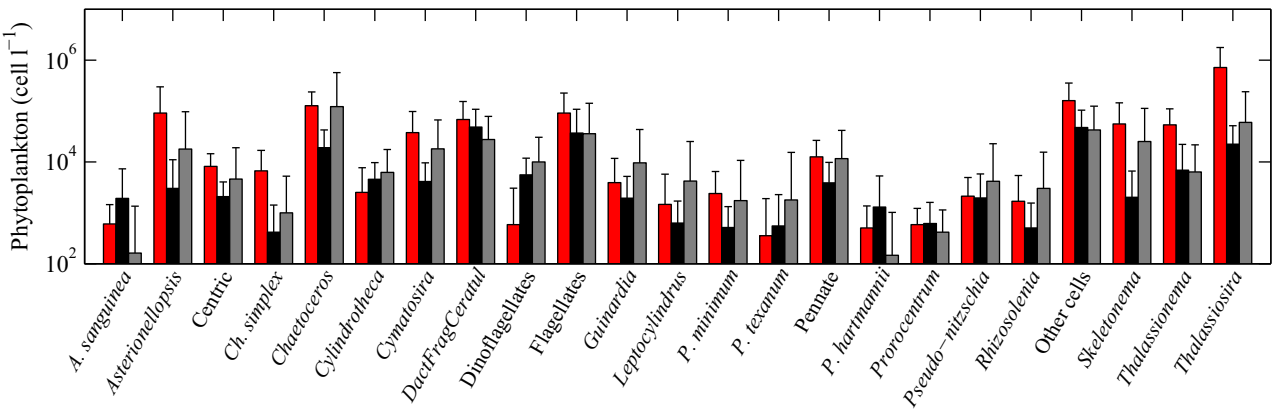

Fig. 5. Time series mean cell abundances and standard deviations of the categories for June–July (red bars), September (black bars) and for the entire five-year IFCB time series (grey bars). [Color figure can be viewed in the online issue, which is available at wileyonlinelibrary.com.]

PCA was applied to each of the two tropical cyclone periods (June–July and September). Each pair of tropical cyclones had combined effects with respect to freshwater discharge and impact on salinity in the Port Aransas Ship Channel (*see* Figs. 3b–c, 4b–c). Therefore, the periods analyzed for the June–July and September events were based on salinity observations and correspond to the time of the first impact to the time when salinity recovered to its pre-cyclone level. For comparison, PCA was also computed for each individual tropical cyclone and for the entire period (i.e., including all tropical cyclones); results were coherent with those we present here (not shown).

As mentioned above, PCA identifies the dominant coherent fluctuations of the phytoplankton categories with respect to the time series mean abundances for the corresponding period. Further, the time series were standardized over the entire IFCB time series, so PCA represent deviations with respect to the standard deviation of each category for the entire IFCB time series. Figure 5 shows the time series mean abundances and standard deviations for each period and for the entire time series. Differences between time series for June–July and the entire time series are significant for all the categories (ANOVA, $p < 0.05$), with the exception of *Guinardia*, *Leptocylindrus*, *Prorocentrum texanum*, Pennate, *Pseudo-nitzschia*, and *Rhizosolenia*. For September, the categories *Chaetoceros simplex*, *Guinardia*, *Leptocylindrus*, *Prorocentrum minimum*, *P. texanum*, and *Pseudo-nitzschia* are not significantly (ANOVA, $p > 0.05$) different from the entire time series.

Figures 6 and 7 show the scores and category loadings for the first three PCA components. The scores of the PCA components indicate the response of the phytoplankton community over time (left panels), and the increase or decrease in abundance of each category according to its corresponding loading (right panels). Positive loading values for a specific category indicate an increase in its abundance when the score increases. In contrast, negative loadings represent a decrease in the abundance when the score increases. Values close to zero indicate that the category does not follow the evolution displayed by the corresponding component. The original (standardized) time series of each period can be well approximated by simple linear combination of the most relevant scores multiplied by their corresponding loadings. To investigate the origin of the phytoplankton community involved in the response (estuarine or coastal), the fluctuations in time of the scores are plotted against outgoing and incoming tide (denoting estuarine and coastal origin, respectively).

The results of the PCA showed that the first three components accounted for 76.6% of the variance in June–July (Fig. 6). The first PCA component, which explained 38.8% of the variability of the phytoplankton community, revealed increases for most of the categories that started progressively 2 d after the increase in freshwater discharge following Alex and reached a notable peak $\sim$ 4.9 d after (Fig. 6a). Increase peaks were mostly coincident with the outgoing tide. As shown in Fig. 6b, the response was dominated by categories with higher positive loadings: the diatoms *Thalassiosira* (maximum cell abundance 7.4×10^6 cells L^{-1}), Flagellates (maximum cell abundance 0.6×10^6 cells L^{-1}), and Other cells (maximum cell abundance 1.4×10^6 cells L^{-1}). The estimated growth rates were 1.1 d^{-1} for *Thalassiosira*, 1.1 d^{-1} for Flagellates, and 0.7 d^{-1} for Other cells. A few categories (Dinoflagellates, *P. texanum*, *Guinardia* and *Rhizosolenia*) experienced a slight decrease (negative loadings) with respect to their time series mean values.

The second PCA component, accounting for 19.2% of the variability, was characterized by marked increases during the storm surges of the tropical cyclones (Alex and Two) and when the salinity started to recover (Fig. 6c). Most of the peaks coincided with incoming tides, except for the first peaks during the storm surges. The categories that increased were mainly diatoms, primarily *Asterionellopsis* and *Skeletonema* (Fig. 6d). The maximum increase peak occurred 2.5 d after the onset of the storm surge for Alex and 0.8 d for

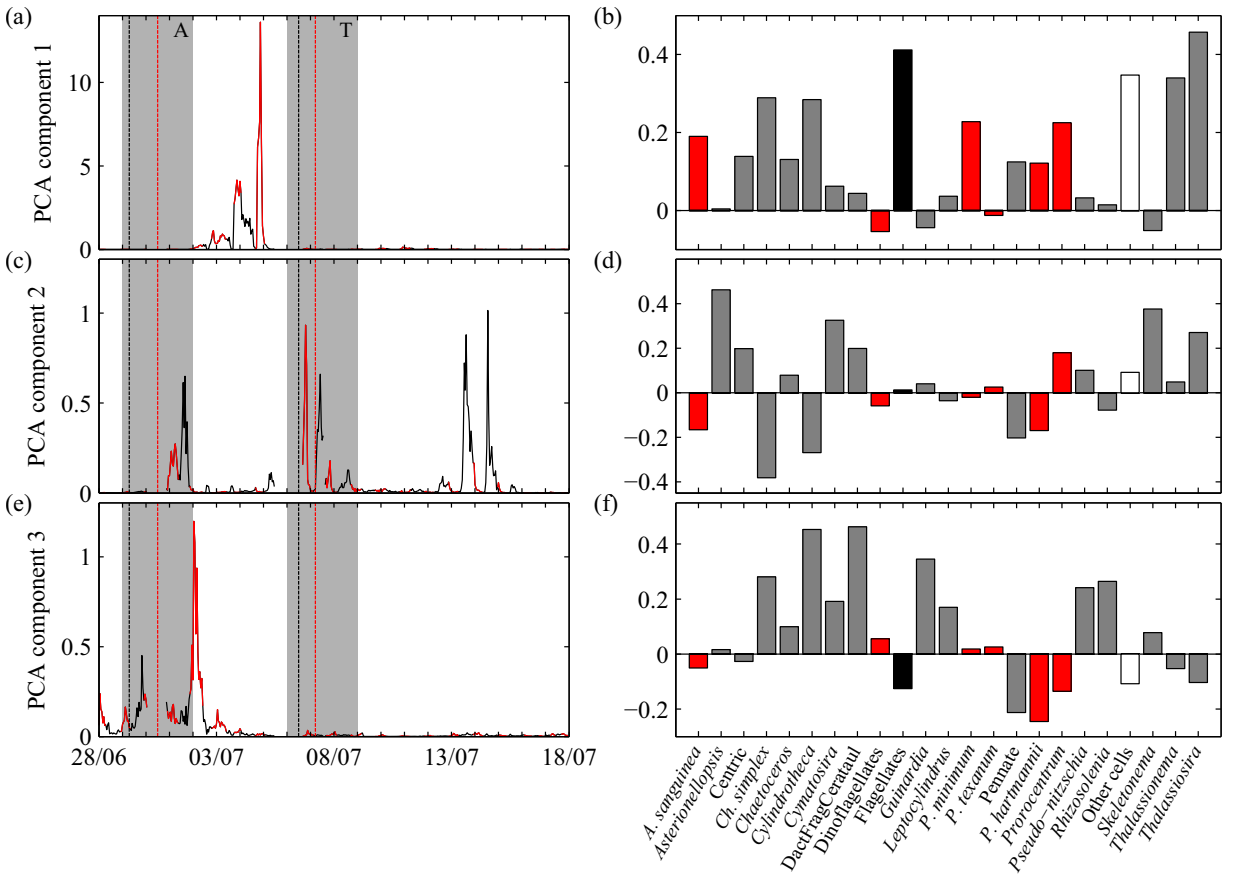

Fig. 6. Results of the first three PCA components for June–July: left panel (a, c and e) PCA scores, where red lines indicate outgoing tide and black lines incoming tide; right panel (b, d, f) category loadings. Red bars indicate dinoflagellates, grey bars indicate diatoms, black bar indicates Flagellates, and white bar indicates Other cells. Note the difference in scale in PCA scores and category loadings. Vertical dashed lines indicate start of the storm surge (black line) and the freshwater discharge (red line) for each tropical cyclone. Grey bars indicate temporal evolution of Hurricane Alex (A) and Tropical Depression Two (T) as in Fig. 2. [Color figure can be viewed in the online issue, which is available at wileyonlinelibrary.com.]

Two. Maximum cell abundances for *Asterionellopsis* were 0.2 $\times$ 10^6 cells L^{-1} during Alex and 0.5 $\times$ 10^6 cells L^{-1} during Two; and for *Skeletonema* were 0.6 $\times$ 10^6 cells L^{-1} during Alex and 0.5 $\times$ 10^6 cells L^{-1} during Two. The estimated growth rates for *Asterionellopsis* were 1.4 d^{-1} and 1.2 d^{-1} during Alex and Two, respectively; and for *Skeletonema* were 1.2 d^{-1} and 1.5 d^{-1}. The categories that decreased during these peaks were the diatoms *C. simplex*, *Cylindrotheca* and Pennate, and all dinoflagellate categories except for *Prorocentrum* and *P. texanum*.

The third PCA component, which accounted for 18.6% of the variability, showed a moderate response 0.8 d after the initiation of the storm surge of Alex and a stronger response 2.9 d after the initiation (Fig. 6e). The first peak was associated with incoming tide and the second with outgoing. Only diatoms, primarily the category DactFragCerataul (*Dactyliosolen fragilissimus*, *Cerataulina pelagica* and *Leptocilyndrus danicus, see* Supporting Information Table S1; maximum cell abundance 3.1 $\times$ 10^5 cells L^{-1}) and *Cylindrotheca* (maximum cell abundance 0.2 $\times$ 10^5 cells L^{-1}) increased notably (Fig. 6f). The calculated growth rates were 1.0 d^{-1} and 1.3 d^{-1}, respectively for both categories. Dinoflagellates did not respond notably or decreased (especially *Polykrikos hartmannii* and *Prorocentrum*). Pennate, Flagellates, and Other cells categories also decreased.

For September, PCA results showed that the first three components accounted for 75.8% of the variance (Fig. 7). Most of the variability of the phytoplankton community was explained by the first component (34.6%), which revealed a modest increase of several categories 4.3 d after the freshwater discharge following Hermine, and a larger increase 6.8 d after the elevated freshwater discharge period following Karl (Fig. 7a,b). Peaks were coincident with both incoming and outgoing tides, but the majority were associated with the latter. The response was dominated by the dinoflagellates *Akashiwo sanguinea* and *P. hartmannii*, but most of the other dinoflagellate categories, Flagellates, Other cells and a few diatoms also increased (Fig. 7b). In the case of Hermine, calculated growth rates for *A. sanguinea* (maximum cell abundance 0.4 $\times$ 10^4 cells L^{-1}) and *P. hartmannii* (maximum cell

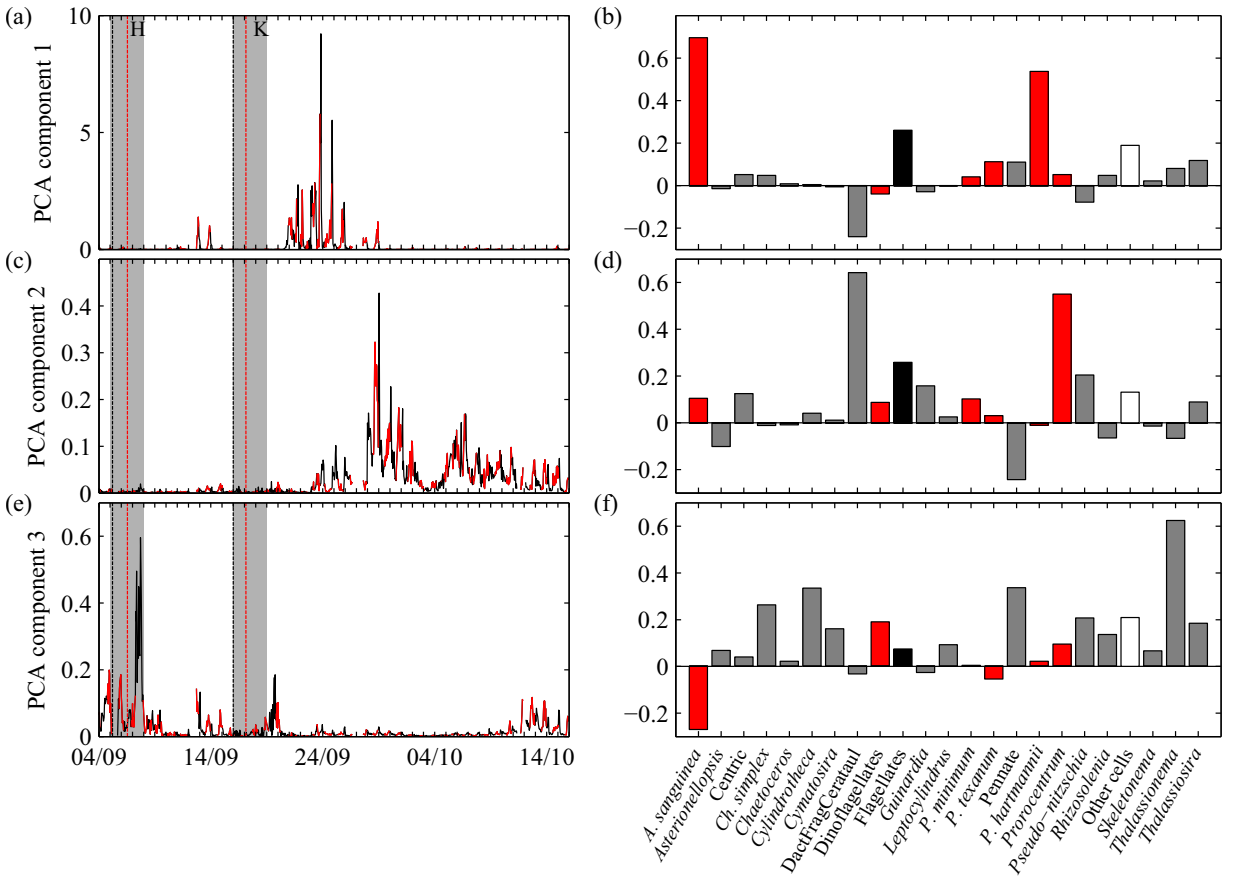

Fig. 7. Results of the first three PCA components for September: left panel (a, c and e) PCA scores, where red lines indicate outgoing tide and black lines incoming tide; right panel (b, d, f) category loadings. Red bars indicate dinoflagellates, grey bars indicate diatoms, black bar indicates Flagellates, and white bar indicates Other cells. Note the difference in scale in PCA scores and category loadings. Vertical dashed lines indicate start of the storm surge (black line) and the freshwater discharge (red line) for each tropical cyclone. Grey bars indicate temporal evolution of Tropical Storm Hermine (H) and Hurricane Karl (K) as in Fig. 2. [Color figure can be viewed in the online issue, which is available at wileyonlinelibrary.com.]

abundance 4.6×10^4 cells L^{-1}) were 0.7 d^{-1} for both species. For Karl, growth rates were 0.8 d^{-1} for *A. sanguinea* (maximum cell abundance 2.8×10^4 cells L^{-1}) and 0.7 d^{-1} for *P. hartmannii* (maximum cell abundance 1.0×10^4 cells L^{-1}). The only category that decreased was DactFragCerataul.

The second PCA component, which accounted for 25.2% of the variability, showed a response pattern that started moderately after the freshwater discharge following Karl reaching maximum values 12 d after, and extended, with a downward trend, during salinity recovery (Fig. 7c). As observed with the first component, most peaks were coincident with outgoing tides. The dominant categories of the response were the diatom DactFragCerataul (maximum cell abundance 2.4×10^5 cells L^{-1}) and the dinoflagellate *Prorocentrum* (maximum cell abundance 0.4×10^4 cells L^{-1}). Estimated growth rates were 0.4 d^{-1} and 0.3 d^{-1} for DactFragCerataul and *Prorocentrum*, respectively. All other dinoflagellate categories, Flagellates, Other cells and a few diatom categories also showed a more moderate increase (Fig. 7d). The categories that decreased or did not respond substantially were mainly diatoms, with Pennate showing the largest decrease.

The third PCA component accounted for 16% of the variability and was characterized by the increase of almost all categories during the storm surges of Hermine and Karl and during salinity recovery (Fig. 7e). The highest increase peaks occurred 4.3 d after the start of the storm surge for Hermine and 6.8 d for Karl. Both peaks corresponded to incoming tides, while other minor peaks corresponded to outgoing tides. The category dominating the response was the diatom *Thalassionema*, and only the dinoflagellate *A. sanguinea* showed a clear decrease (Fig. 7f). Estimated growth rates for *Thalassionema* (maximum cell abundance 1.4×10^5 cells L^{-1} and 0.7×10^5 cells L^{-1} for Hermine and Karl, respectively) were 0.9 d^{-1} for both tropical cyclones.

Discussion

Phytoplankton community responses to environmental changes associated with episodic perturbations such as

tropical cyclones can occur rapidly. To our knowledge, this study is the first to report the effect of tropical cyclones on phytoplankton community composition over the course of their passage and aftermath with high temporal resolution (hours). This is mainly because of the episodic nature of tropical cyclones and the lack of observational tools capable of characterizing phytoplankton communities at the appropriate temporal resolution. With the high-frequency measurements provided by the IFCB, we were able to capture and quantify the short-term responses (hours–days) of the phytoplankton community related to tropical cyclones in an estuarine-coastal system. We first discuss the possible causes of the responses and their relation to the cyclone characteristics. Next, we examine the responses at the community composition level, and finally we discuss the implications of our findings in a larger context.

Causes of phytoplankton responses to the tropical cyclones

Tropical cyclones produced two major impacts in the physical conditions of the studied area. First, the strong onshore winds during the passage of the cyclones caused storm surges. Afterward, heavy rains produced a substantial increase in freshwater discharge. The PCA suggests that phytoplankton responded to both processes. The phytoplankton peaks lagged the onset of storm surges by 0.8-3.6 d and the freshwater discharges by 4.9-12 d. The estimated growth rates for the dominant categories in each response (0.8-1.5 d^{-1} for the storm surges and 0.3-1.1 d^{-1} for the freshwater discharges) agree with the values reported in the literature for the taxa considered (Karentz and Smayda 1984; Collos 1986; Furnas 1990; Crosbie and Furnas 2001; Litchman et al. 2007; Matsubara et al. 2007). This confirms the correspondence between the phytoplanton response and the corresponding stimulating process.

Previous studies have shown that phytoplankton increases in coastal and estuarine systems during the passage of tropical cyclones occur as a result of nutrient entrainment caused by wind-forced upwelling, water mixing, and sediment resuspension (e.g., Fogel et al. 1999; Shiah et al. 2000; Paerl et al. 2006*b*). Nutrient pulses can enhance phytoplankton concentrations within a few hours (Collos 1986; Pinckney et al. 1999). Unfortunately, nutrient data were collected only once a month at the Mission-Aransas NERR, and did not coincide with the tropical cyclone occurrences, so could not capture the short-term impact on nutrient concentrations. However, the rapid responses by the phytoplankton to the storm surges suggest growth of the phytoplankton community is due to nutrient enhancement. Storm surge, in combination with strong winds, can cause substantial sediment resuspension. The responses of the phytoplankton community to the storm surges showed increases first during incoming tides (Figs. 6c, 7e), indicating that environmental conditions were conducive for phytoplankton growth in nearshore waters outside the estuary. The second increases in the phytoplankton response to the storm surge were associated with outgoing tides (Fig. 6c,e), supporting the observation that conditions inside the estuary were also favorable for growth.

The phytoplankton community also showed responses associated with the freshwater discharges after the passage of the tropical cyclones. These responses were greater than those during storm surge. The peaks in the responses were coincident with outgoing tides, which suggests favorable conditions for phytoplankton growth inside the estuary. Numerous publications describe increases in phytoplankton biomass and changes in the community composition triggered by nutrient supply due to freshwater inflow related to tropical cyclones (e.g., Mallin et al. 1993; Paerl et al. 2001, 2006*a*). Indeed, there was elevated nutrient loading through river runoff after these tropical cyclone events in the Mission-Aransas estuary ($\sim$ 1300−2700 kg d^{-1} of nitrate + nitrite and $\sim$ 90−550 kg d^{-1} of ammonium; Bruesewitz et al. 2013; Turner et al. 2014). Therefore, increased nutrient input into the estuaries associated with freshwater discharge was a likely cause for the observed increases in cell abundances.

The impacts of tropical cyclones on phytoplankton are variable and depend on cyclone characteristics, on proximity of landfall location, and on environmental conditions of the system both before and after the passage of the tropical cyclone (Mallin et al. 2002; Mallin and Corbett 2006; Wetz and Paerl 2008*a*). Our results show definite phytoplankton responses both during and after the passage of the four tropical cyclones, although responses varied. Storm surges associated with the passage of the cyclones induced responses at community level for all cyclones, but were more notable during Alex, Two and Hermine. Although Hurricane Karl was one of the more intense cyclones (along with Alex), the landfall location was the farthest from the study area (Fig. 1a). This likely weakened the impact of Karl on the phytoplankton community during the storm surge at our study site. Another possibility is a role of light limitation due to sediment resuspension reducing phytoplankton growth. We can discount this effect, however, because maximum turbidity values in the Port Aransas Ship Channel were registered during the passage of Alex and they were much lower during Karl (data not shown).

Total cell abundance maxima occurred after Hurricane Alex (10.3×10^6 cells L^{-1}) and Hurricane Karl (1.2×10^6 cells L^{-1}) in response to the freshwater discharge for each pair of tropical cyclones. In contrast, cell abundances did not show a clear increase following Two and Hermine. This suggests a relationship between cyclone intensity and total phytoplankton abundance. It is plausible that the input of nutrients through the moderate river discharge after Two was not sufficient to trigger notable responses in the phytoplankton community at our study site, as reported in other estuaries (Paerl et al. 2006*a*,*b*; Wetz and Paerl 2008*a*).

However, the freshwater discharge after Hermine was the highest of the four tropical cyclones. Rapid flushing due to elevated freshwater inflow can result in unfavorable conditions for marine phytoplankton growth and in transport of phytoplankton cells (Paerl et al. 1998; Peierls et al. 2003). The rapid decrease in salinity after the river discharge following Hermine suggested increased flushing in the estuary, which may have restricted the buildup of phytoplankton biomass.

Responses at the community composition level

Examination of the categories involved in the different response patterns of the phytoplankton community allowed for a more detailed understanding of the variability in the community composition in relation to the effects of the tropical cyclones. Responses during the passage of the tropical cyclones were mainly dominated by diatoms. Diatoms are fast-growing taxa known to respond rapidly to nutrient input (Collos 1986; Pinckney et al. 1999). Particularly during the passage of Alex, we observed a considerable number of responses in the community composition within a very short period (0.8-3.6 d). The response during the storm surge caused by this hurricane (Fig. 6c) showed a marked increase in cell abundance that consisted predominantly of the diatoms *Asterionellopsis* and *Skeletonema* (Fig. 6d). *Asterionellopsis* and *Skeletonema* are common in coastal neritic waters, and *Skeletonema* has been reported to be dominant after a hurricane where upwelling was a nutrient source (Tsuchiya et al. 2013). These taxa are able to grow rapidly under favorable conditions and have among the highest growth rates measured for diatoms both in situ and in laboratory cultures (1.3-2.9 d^{-1} and 0.7-4.3 d^{-1} for *Asterionellopsis* and *Skeletonema*, respectively; Karentz and Smayda 1984; Furnas 1990). Moreover, there was a moderate increase in *Cymatosira*, a typical benthic diatom, which could be an indication of resuspension (Hasle and Syvertsen 1997). Therefore, the increase of these categories together with their association with incoming tides supports our assumption that conditions in nearshore waters outside the estuary were favorable for phytoplankton growth as a result of nutrient entrainment. Shortly after (0.4 d) and coinciding with outgoing tides, the community shifted and was characterized by the increases in the categories DactFragCerataul and *Cylindrotheca* (Fig. 6e,f). Species included in DactFragCerataul have high in situ and laboratory growth rates ranging between 0.4 d^{-1} and 1.9 d^{-1} (Karentz and Smayda 1984; Furnas 1990; Crosbie and Furnas 2001). *Cylindrotheca* is an estuarine diatom planktonic and epipelic (mud-inhabiting) with high in situ growth rates (0.5-3.3 d^{-1}; Furnas 1990; Crosbie and Furnas 2001), and therefore the observed increase could indicate growth after resuspension. This reinforces the idea that the storm surge also resuspended nutrients inside the estuary, which favored the rapid growth of these diatom taxa.

The response during the passage of Two showed an increase of the same diatoms observed during the passage of the previous hurricane, Alex (Fig. 6c,d). As mentioned above, the species dominating the response (*Asterionellopsis* and *Skeletonema*) were characteristic of coastal neritic and upwelling regions. The maximum peak of the response, however, coincided with incoming tide. It should be noted that there is a data gap before this peak, hampering the interpretation of the observations. The community response to the storm surges of the tropical cyclones in September (Hermine and Karl) was also dominated by diatoms (Fig. 7e,f), although the primary species were different than those during June–July (mainly *Thalassionema*). *Thalassionema* is a coastal neritic diatom found in upwelling regions with high in situ and laboratory growth rates (0.6-1.8 d^{-1}; Karentz and Smayda 1984; Crosbie and Furnas 1990). We note that the very high growth rates of the diatom taxa that dominated the responses to the storm surges are in agreement with our estimated growth rates.

Freshwater discharges associated with the tropical cyclones also triggered notable responses in the phytoplankton community composition; however, these were characterized by different species and taxonomic groups. In general, the response to freshwater input showed an increase of dinoflagellates, Flagellates and Other cells. In the case of Alex, increases in a large number of diatoms were also observed. Increase of dinoflagellates shortly after high freshwater inflows following tropical cyclones has been reported in previous studies (Zeeman 1985; Tsuchiya et al. 2013). This shift seems to be related to the ability of dinoflagellates to assimilate organic compounds together with the high input of these substrates from river runoff. Flagellates and Other cells were the secondary groups that contributed to the community response. A visual inspection of the images revealed that Flagellates and Other cells included a substantial proportion of prasinophytes, euglenophytes and cryptophytes, which are fast-growing phytoplankton groups that respond rapidly to nutrient enrichment associated with freshwater inflow and under reduced salinity conditions (e.g., Pinckney et al. 1999; Paerl et al. 2006*b*, 2010). These taxa have maximum growth rates ranging between 1.3 d^{-1} and 1.6 d^{-1} (Litchman et al. 2007). The response to the discharge after Hermine and Karl was dominated by two dinoflagellate categories, *A. sanguinea* and *P. hartmannii* (Fig. 7a,b), both common estuarine species (e.g., Badylak and Phlips 2004; Rothenberger et al. 2009; Phlips et al. 2010). *A. sanguinea* can sustain growth rates up to 1.1 d^{-1} (Matsubara et al. 2007). In contrast, although dinoflagellates increased during the discharge period following Alex, the community response was dominated by a genus of diatoms (*Thalassiosira*; Fig. 6a,b). *Thalassiosira* is typically found in a wide range of habitats and exhibits high growth rates (0.8-2.6 d^{-1}; Karentz and Smayda 1984; Furnas 1990; Crosbie and Furnas 2001). It should be noted that the second, more

moderate response after the freshwater discharge in September (PCA component 2; Fig. 7c,d) was dominated by another diatom category, DactFragCerataul. The freshwater discharge that resulted from the rainfall after the tropical cyclones, caused very high loading of dissolved organic nitrogen (DON) to the Mission-Aransas estuary, with maximum values reached after Karl ($\sim$ 700–12500 kg d^{-1} of DON; Bruesewitz et al. 2013; Turner et al. 2014). Dinoflagellates are physiologically well suited to benefit from organic N forms (Bronk et al. 2007; Dagenais-Bellefeuille and Morse 2013, and references therein), which confers a competitive advantage in organic N-rich environments. Thus, dinoflagellate species likely responded more notably than fast-growing phytoplankton groups such as diatoms and small flagellates. Diatoms, on the other hand, are known to take advantage of large and episodic inputs of inorganic N for rapid growth, rather than from organic compounds (Bronk et al. 2007; Wawrik et al. 2009). In addition, some diatom species have the capacity for intracellular nutrient storage that allows them to keep dividing long after nutrient uptake, which represents an ecological advantage with respect to other phytoplankton groups, including dinoflagellates (Collos 1986; Pinckney et al. 1999). In particular, *Thalassiosira* shows time lags between nutrient pulses and cell division of up to 72 h due to its capability of internal nutrient accumulation (Collos 1986). Similarly, species of *Dactyliosolen* and *Cerataulina* (species included in DactFragCerataul) have been reported to bloom in nutrient-pulsed environments as a result of an ecological strategy favored by nutrient storage ability (Phlips et al. 2010). This ecological strategy may explain the dominance of *Thalassiosira* and DactFragCerataul in the community response after the freshwater discharge following Alex and Karl, respectively. As observed in responses to the storm surges, the growth rates estimated for the categories that dominated the responses to freshwater discharges are in accordance with those reported in the literature.

Potential implications in ecosystem functioning

Previous reports have shown increases in phytoplankton biomass shortly after (< 1 week) the passage of a tropical cyclone (Miller et al. 2006; Paerl et al. 2006*b*; Wetz and Paerl 2008*a*; Tsuchiya et al. 2013). Indeed, in our study we observed a significant phytoplankton bloom that reached its maximum abundance 4.9 d after the passage of hurricane Alex. Utilizing the IFCB, we were able to determine that the bloom was dominated primarily by *Thalassiosira*, which reached abundances up to 7.4×10^6 cells L^{-1}. Based on the IFCB time series at TOAST, this bloom was the largest ever recorded for *Thalassiosira*. In addition, the occurrence of a *Thalassiosira* bloom in July was rare, since the highest abundances were usually observed during winter–spring months (December–April). A previous study in the Neuse River also reported higher abundance of *Thalassiosira* during years with hurricanes (Rothenberger et al. 2009); however, these high abundances occurred during the typical season (winter–spring). Similarly, the notable increases in cell abundance of the dinoflagellates *A. sanguinea* and *P. hartmannii* detected during the discharges after the September tropical cyclones, although modest compared to *Thalassiosira*, were also the maximum abundances observed for both of these species.

In estuarine and coastal ecosystems, pulsed nutrient inputs can alter the plankton community structure, with implications for ecosystem functioning and health. Rapid, short-term changes in phytoplankton composition like the ones observed in the present study can influence the composition of the grazer communities, and by extension of higher trophic levels (Zhang and Wang 2000; Hoover et al. 2006). In addition, the type of N supplied can further influence the trophic interactions through the promotion of blooms of specific phytoplankton groups. For example, dinoflagellates, which appear to be stimulated by organic N forms, are considered to have less nutritional value compared to diatoms, or are less preferred as food (Sterner and Schulz 1998). Although further study is required to determine whether the observed deviations produced positive or negative effects on trophic transfers and their efficiency, it is clear that tropical cyclone events exerted changes on the phytoplankton community in our study area, and consequently, potentially to ecosystem functioning.

Conclusions

The detailed taxonomic time series of phytoplankton community composition from the IFCB provides essential knowledge on the responses of the phytoplankton community to tropical cyclones at the relevant ecosystem time scale. Moreover, it reports baseline information on the effects of tropical cyclones in an estuarine and coastal system from the Western Gulf of Mexico. The high-frequency measurements of the IFCB allowed for the detection of short-term responses (hours–days) of the phytoplankton community, which would have been undetected with the typical low-frequency samplings. Some shifts in the community structure were of very short duration (a few days), but such short-term events can affect higher trophic levels (e.g., Zhang and Wang 2000; Hoover et al. 2006; Wetz and Paerl 2008*b*). The potential for rapid responses emphasizes the need for high-resolution sampling to fully capture the effects of these perturbations on the ecosystem. In addition, the location of the IFCB at the entrance to the estuary permited identification of phytoplankton responses both in the estuarine system and in the nearshore coastal waters. These observations underscore the potential of tropical cyclones to alter the phytoplankton community of both types of ecosystems. Deployment of additional instruments to increase spatial resolution within this coastal system would help to distinguish the responses of the estuarine and nearshore ecosystems.

The alterations in the phytoplankton community caused by the tropical cyclones produced significant deviations for most analyzed taxa from 2008 to 2012 averages. This implies that we have to be very cautious when extracting global signals of climate change from phytoplankton observations in coastal and estuarine ecosystems where episodic processes like tropical cyclones can mask tendencies induced by changing climate (Cloern and Jassby 2008). In addition, some of the species that were involved in the responses to the tropical cyclones, *A. sanguinea* and *P. hartmannii*, are toxic species (Cardwell et al. 1979; Tang et al. 2013). Other studies reported the occurrence of toxic species following a hurricane (Hall et al. 2008). The few tropical cyclones analyzed in our study do not allow us to determine if occurrence of harmful algal blooms will be enhanced by the predicted increase in tropical cyclone frequency in the future. The physical and hydrological impacts and the resulting effect in phytoplankton were unique for each tropical cyclone, as has been reported in the literature (e.g., Mallin et al. 2002; Paerl et al. 2006*b*). The majority of studies, based on chlorophyll *a* or analysis of other pigments, showed either lack of phytoplankton response or development of phytoplankton blooms of diverse magnitude and duration. Our study of four sequential tropical cyclones supports these observations, and the taxonomic resolution provided by the IFCB also revealed that the taxa dominating each of the responses were different among the tropical cyclones despite occurring within a relatively short period of time.

References

Babin, S., J. Carton, T. Dickey, and J. Wiggert. 2004. Satellite evidence of hurricane-induced phytoplankton blooms in an oceanic desert. J. Geophys. Res. **109**: C03043. doi:10.1029/2003JC001938

Badylak, S., and E. Phlips. 2004. Spatial and temporal patterns of phytoplankton composition in subtropical coastal lagoon, the Indian River Lagoon, Florida, USA. J. Plankton Res. **26**: 1229-1247. doi:10.1093/plankt/fbh114

Breiman, L. 2001. Random forests. Machine Learning **45**: 5-32. doi:10.1023/A:1010933404324

Bronk, D., J. See, P. Bradley, and L. Killberg. 2007. DON as a source of bioavailable nitrogen for phytoplankton. Biogeosciences **4**: 283-296. doi:10.5194/bg-4-283-2007

Brown, C. A., G. A. Jackson, and D. A. Brooks. 2000. Particle transport through a narrow tidal inlet due to tidal forcing and implications for larval transport. J. Geophys. Res. Oceans (1978-2012) **105**: 24141-24156. doi:10.1029/2000JC000211

Bruesewitz, D. A., W. S. Gardner, R. F. Mooney, L. Pollard, and E. J. Buskey. 2013. Estuarine ecosystem function response to flood and drought in a shallow, semiarid estuary: Nitrogen cycling and ecosystem metabolism. Limnol. Oceanogr. **58**: 2293-2309. doi:10.4319/lo.2013.58.6.2293

Campbell, L., D. W. Henrichs, R. J. Olson, and H. M. Sosik. 2013. Continuous automated imaging-in-flow cytometry for detection and early warning of *Karenia brevis* blooms in the Gulf of Mexico. Environ. Sci. Pollut. Res. **20**: 6896-6902. doi:10.1007/s11356-012-1437-4

Campbell, L., R. Olson, H. Sosik, A. Abraham, D. Henrichs, and C. Hyatt. 2010. First harmful *Dinophysis* (Dinophyceae, Dinophysiales) bloom in the US is revealed by Automated Imaging Flow Cytometry. J. Phycol. **46**: 66-75. doi:10.1111/j.1529-8817.2009.00791.x

Cardwell, R. D., S. Olsen, M. I. Carr, and E. W. Sanborn. 1979. Causes of oyster larvae mortality in south Puget Sound, p. 73, NOAA technical memorandum ERL MESA-39. Marine Ecosystems Analysis Program [Office], Environmental Research Laboratories.

Cloern, J. E., and A. D. Jassby. 2008. Complex seasonal patterns of primary producers at the land-sea interface. Ecol. Lett. **11**: 1294-1303. doi:10.1111/j.1461-0248.2008.01244.x

Collos, Y. 1986. Time-lag algal growth dynamics: Biological constraints on primary production in aquatic environments. Mar. Ecol. Prog. Ser. **33**: 193-206. doi:10.3354/meps033193

Crosbie, N. D., and M. J. Furnas. 2001. Net growth rates of picocyanobacteria and nano-/microphytoplankton inhabiting shelf waters of the central (17°S) and southern (20°S) Great Barrier Reef. Aquat. Microb. Ecol. **24**: 209-224. doi:10.3354/ame024209

Dagenais-Bellefeuille, S., and D. Morse. 2013. Putting the N in dinoflagellates. Front. Microbiol. **4**: Article 369. doi:10.3389/fmicb.2013.00369

Dee, D., and others. 2011. The ERA-Interim reanalysis: Configuration and performance of the data assimilation system. Q. J. R. Meteorol. Soc. **137**: 553-597. doi:10.1002/qj.828

Fogel, M. L., C. Aguilar, R. Cuhel, D. J. Hollander, J. D. Willey, and H. W. Paerl. 1999. Biological and isotopic changes in coastal waters induced by Hurricane Gordon. Limnol. Oceanogr. **44**: 1359-1369. doi:10.4319/lo.1999.44.6.1359

Furnas, M. J. 1990. In situ growth rates of marine phytoplankton: Approaches to measurement, community and species growth rates. J. Plankton Res. **12**: 1117-1151. doi:10.1093/plankt/12.6.1117

Harred, L. B., and L. Campbell. 2014. Predicting harmful algal blooms: A case study with *Dinophysis ovum* in the Gulf of Mexico. J. Plankton Res. **36**: 1434-1445. doi:10.1093/plankt/fbu070

Hasle, G. R., and E. E. Syvertsen. 1997. Marine diatoms, p. 5-385. *In* C. R. Tomas [ed.], Identifying marine phytoplankton. Academic Press.

Henrichs, D. W., H. M. Sosik, R. J. Olson, and L. Campbell. 2011. Phylogenetic analysis of *Brachidinium capitatum* (Dinophyceae) from the Gulf of Mexico indicates membership in the Kareniaceae. J. Phycol. **47**: 366-374. doi:10.1111/j.1529-8817.2011.00960.x

Holland, J., N. Maciolek, R. Kalke, L. Mullins, and C. Oppenheimer. 1975. A benthos and plankton study of the

Corpus Christi, Copano and Aransas Bay systems, p. 174. Texas Water Development Board. University of Texas Port Aransas Marine Laboratory.

Hoover, R., D. Hoover, M. Miller, M. Landry, E. Decarlo, and F. Mackenzie. 2006. Zooplankton response to storm runoff in a tropical estuary: Bottom-up and top-down controls. Mar. Ecol. Prog. Ser. **318**: 187-201. doi:10.3354/meps318187

Hotelling, H. 1933. Analysis of a complex of statistical variables into principal components. J. Educ. Psychol. **24**: 417-441. doi:10.1037/h0071325

Hu, C., and F. E. Muller-Karger. 2007. Response of sea surface properties to Hurricane Dennis in the eastern Gulf of Mexico. Geophys. Res. Lett. **34**: L07606. doi:10.1029/2006GL028935

Karentz, D., and T. J. Smayda. 1984. Temperature and seasonal occurrence patterns of 30 dominant phytoplankton species in Narragansett Bay over a 22-year period (1959-1980). Mar. Ecol. Prog. Ser. **18**: 277-293. doi:10.3354/meps018277

Leffler, K. E., and D. A. Jay. 2009. Enhancing tidal harmonic analysis: Robust (hybrid L1/L2) solutions. Cont. Shelf Res. **29**: 78-88. doi:10.1016/j.csr.2008.04.011

Lin, I., and others 2003. New evidence for enhanced ocean primary production triggered by tropical cyclone. Geophys. Res. Lett. **30**: 1718. doi:10.1029/2003GL017141

Litchman, E., C. A. Klausmeier, O. M. Schofield, and P. G. Falkowski. 2007. The role of functional traits and trade-offs in structuring phytoplankton communities: Scaling from cellular to ecosystem level. Ecol. Lett. **10**: 1170-1181. doi:10.1111/j.1461-0248.2007.01117.x

Mallin, M. A., and C. A. Corbett. 2006. How hurricane attributes determine the extent of environmental effects: Multiple hurricanes and different coastal systems. Estuaries Coasts **29**: 1046-1061. doi:10.1007/BF02798667

Mallin, M. A., H. W. Paerl, J. Rudek, and P. W. Bates. 1993. Regulation of estuarine primary production by watershed rainfall and river flow. Mar. Ecol. Prog. Ser. **93**: 199-203. doi:10.3354/meps093199

Mallin, M. A., M. H. Posey, M. R. Mciver, D. C. Parsons, S. H. Ensign, and T. D. Alphin. 2002. Impacts and recovery from multiple hurricanes in a Piedmont–Coastal Plain river system human development of floodplains greatly compounds the impacts of hurricanes on water quality and aquatic life. BioScience **52**: 999-1010. doi:10.1641/0006-3568(2002)052[0999:IARFMH]2.0.CO;2

Matsubara, T., S. Nagasoe, Y. Yamasaki, T. Shikata, Y. Shimasaki, Y. Oshima, and T. Honjo. 2007. Effects of temperature, salinity, and irradiance on the growth of the dinoflagellate *Akashiwo sanguinea*. J. Exp. Mar. Biol. Ecol. **342**: 226-230. doi:10.1016/j.jembe.2006.09.013

Meehl, G., and others. 2007. Global climate projections, p. 747-846. *In* S. Solomon and others [eds.], Climate Change 2007: The Physical Science Basis. Contribution of Working Group I to the Fourth Assessment Report of the Intergovernmental Panel on Climate Change. Cambridge Univ. Press.

Miller, W. D., L. W. Harding, and J. E. Adolf. 2006. Hurricane Isabel generated an unusual fall bloom in Chesapeake Bay. Geophys. Res. Lett. **33**: L06612. doi:10.1029/2005GL025658

Mooney, R. F., and J. W. McClelland. 2012. Watershed export events and ecosystem responses in the Mission–Aransas National Estuarine Research Reserve, South Texas. Estuaries Coasts **35**: 1468-1485. doi:10.1007/s12237-012-9537-4

Murrell, M. C., J. D. Hagy, E. M. Lores, and R. M. Greene. 2007. Phytoplankton production and nutrient distributions in a subtropical estuary: Importance of freshwater flow. Estuaries Coasts **30**: 390-402. doi:10.1007/BF02819386

Olson, R., and H. Sosik. 2007. A submersible imaging-in-flow instrument to analyze nano-and microplankton: Imaging FlowCytobot. Limnol. Oceanogr.: Methods **5**: 195-203. doi:10.4319/lom.2007.5.195

Orlando, S. P., L. P. Rozas, G. H. Ward, and C. J. Klein. 1993. Salinity characteristics of Gulf of Mexico estuaries, p. 209. Silver Spring, MD: National Oceanic and Atmospheric Administration, Office of Ocean Resources Conservation and Assessment.

Paerl, H. W., J. L. Pinckney, J. M. Fear, and B. L. Peierls. 1998. Ecosystem responses to internal and watershed organic matter loading: Consequences for hypoxia in the eutrophying Neuse River Estuary, North Carolina, USA. Mar. Ecol. Prog. Ser. **166**: 17-25. doi:10.3354/meps166017

Paerl, H. W., K. L. Rossignol, S. N. Hall, B. L. Peierls, and M. S. Wetz. 2010. Phytoplankton community indicators of short-and long-term ecological change in the anthropogenically and climatically impacted Neuse River Estuary, North Carolina, USA. Estuaries Coasts **33**: 485-497. doi:10.1007/s12237-009-9137-0

Paerl, H. W., L. M. Valdes, B. L. Peierls, J. E. Adolf, and L. W. Harding, Jr. 2006b. Anthropogenic and climatic influences on the eutrophication of large estuarine ecosystems. Limnol. Oceanogr. **51**: 448-462. doi:10.4319/lo.2006.51.1_part_2.0448

Paerl, H. W., and others. 2001. Ecosystem impacts of three sequential hurricanes (Dennis, Floyd, and Irene) on the United States' largest lagoonal estuary, Pamlico Sound, NC. Proc. Natl. Acad. Sci. **98**: 5655-5660. doi:10.1073/pnas.101097398

Paerl, H. W., and others. 2006a. Ecological response to hurricane events in the Pamlico Sound system, North Carolina, and implications for assessment and management in a regime of increased frequency. Estuaries Coasts **29**: 1033-1045. doi:10.1007/BF02798666

Peierls, B. L., R. R. Christian, and H. W. Paerl. 2003. Water quality and phytoplankton as indicators of hurricane impacts on a large estuarine ecosystem. Estuaries **26**: 1329-1343. doi:10.1007/BF02803635

Pennock, J. R. 1999. Nutrient behavior and phytoplankton production in Gulf of Mexico Estuaries, p. 109-162. *In* T.

S. Bianchi, J. R. Pennock and R. R. Twilley [eds.], Biogeochemistry of Gulf of Mexico estuaries. Wiley.

Phlips, E. J., S. Badylak, M. C. Christman, and M. A. Lasi. 2010. Climatic trends and temporal patterns of phytoplankton composition, abundance, and succession in the Indian River Lagoon, Florida, USA. Estuaries Coasts **33**: 498-512. doi:10.1007/s12237-009-9166-8

Phlips, E. J., and others. 2012. Climatic influences on autochthonous and allochthonous phytoplankton blooms in a subtropical estuary, St. Lucie Estuary, Florida, USA. Estuaries Coasts **35**: 335-352. doi:10.1007/s12237-011-9442-2

Pinckney, J. L., H. W. Paerl, and M. B. Harrington. 1999. Responses of the phytoplankton community growth rate to nutrient pulses in variable estuarine environments. J. Phycol. **35**: 1455-1463. doi:10.1046/j.1529-8817.1999.3561455.x

Reynolds, C. S. 2006. Ecology of phytoplankton. Cambridge Univ. Press.

Rothenberger, M. B., J. M. Burkholder, and T. R. Wentworth. 2009. Use of long-term data and multivariate ordination techniques to identify environmental factors governing estuarine phytoplankton species dynamics. Limnol. Oceanogr. **54**: 2107-2127. doi:10.4319/lo.2009.54.6.2107

Shiah, F.-K., S.-W. Chung, S.-J. Kao, G.-C. Gong, and K.-K. Liu. 2000. Biological and hydrographical responses to tropical cyclones (typhoons) in the continental shelf of the Taiwan Strait. Cont. Shelf Res. **20**: 2029-2044. doi: 10.1016/S0278-4343(00)00055-8

Sosik, H., and R. Olson. 2007. Automated taxonomic classification of phytoplankton sampled with imaging-in-flow cytometry. Limnol. Oceanogr.: Methods **5**: 204-216. doi: 10.4319/lom.2007.5.204

Sterner, R. W., and K. L. Schulz. 1998. Zooplankton nutrition: recent progress and a reality check. Aquat. Ecol. **32**: 261-279. doi:10.1023/A:1009949400573

Tang, Y. Z., M. J. Harke, and C. J. Gobler. 2013. Morphology, phylogeny, dynamics, and ichthyotoxicity of *Pheopolykrikos hartmannii* (Dinophyceae) isolates and blooms from New York, USA. J. Phycol. **49**: 1084-1094. doi:10.1111/jpy.12114

Tsuchiya, K., and others. 2013. Phytoplankton community response and succession in relation to typhoon passages in the coastal waters of Japan. J. Plankton Res. **36**: 424–438. doi:10.1093/plankt/fbt1127.

Turner, E. L., D. A. Bruesewitz, R. F. Mooney, P. A. Montagna, J. W. McClelland, A. Sadovskia, E. J. Buskey. 2014. Comparing performance of five nutrient phytoplankton zooplankton (NPZ) models in coastal lagoons. Ecol. Model. **277**: 13-26. doi:10.1016/j.ecolmodel.2014.01.007

Wawrik, B., A. V. Callaghan, and D. A. Bronk. 2009. Use of inorganic and organic nitrogen by *Synechococcus* spp. and diatoms on the West Florida Shelf as measured using stable isotope probing. Appl. Environ. Microb. **75**: 6662-6670. doi:10.1128/AEM.01002-09

Wetz, M. S., and H. W. Paerl. 2008a. Impact of large storm events with different meteorological characteristics on estuarine ciliate biomass. J. Plankton Res. **30**: 551-557. doi:10.1093/plankt/fbn020.

Wetz, M. S., and H. W. Paerl. 2008b. Estuarine phytoplankton responses to hurricanes and tropical storms with different characteristics (trajectory, rainfall, winds). Estuaries Coasts **31**: 419-429. doi:10.1007/s12237-008-9034-y

Wetz, M. S., and D. W. Yoskowitz. 2013. An 'extreme' future for estuaries? Effects of extreme climatic events on estuarine water quality and ecology. Mar. Pollut. Bull. **69**: 7-18. doi:10.1016/j.marpolbul.2013.01.020][23474351

Wynne, T. T., R. P. Stumpf, M. C. Tomlinson, V. Ransibrahmanakul, and T. A. Villareal. 2005. Detecting *Karenia brevis* blooms and algal resuspension in the western Gulf of Mexico with satellite ocean color imagery. Harmful Algae **4**: 992-1003. doi:10.1016/j.hal.2005.02.004

Yuan, J., R. L. Miller, R. T. Powell, and M. J. Dagg. 2004. Storm-induced injection of the Mississippi River plume into the open Gulf of Mexico. Geophys. Res. Lett. **31**: L09312. doi:10.1029/2003GL019335

Zeeman, S. I. 1985. The effects of tropical storm Dennis on coastal phytoplankton. Estuar. Coast. Shelf Sci. **20**: 403-418. doi:10.1016/0272-7714(85)90085-X

Zhang, W., and R. Wang. 2000. Rapid changes in stocks of ciliate microzoo-plankton associated with a hurricane in the Bohai Sea (China). Aquat. Microb. Ecol. **23**: 97-101. doi:10.3354/ame023097

Acknowledgments

We thank the members of the Campbell laboratory for help with IFCB data processing, and the Buskey laboratory (University of Texas Marine Science Institute) for IFCB assistance. We also thank two anonymous reviewers for their helpful comments. We thank E. Buskey and the Mission-Aransas NERR program, the National Oceanic and Atmospheric Administration, the U.S. Geological Survey, and the Texas A&M University Corpus Christi Division of Nearshore Research for providing the environmental data used in this study. This is ECOHAB contribution #827. This research was supported by grants from a Marie Curie International Outgoing Fellowship within the 7th European Community Framework Programme (GA-302562) and from the National Oceanographic and Atmospheric Administration/Ecology of Harmful Algal Bloom program (NOAA/ECOHAB NA09NOS4780196). A. J. was supported by a Ramón y Cajal grant from the Spanish Ministry of Economy and Competitiveness.

Submitted 16 January 2015
Revised 7 April 2015
Accepted 30 April 2015

Associate editor: Anya Waite